

Response to David De Vleeschouwer's comment

We thank David De Vleeschouwer for his comments considering the comparison of our sensitivity analysis of the Devonian climate to orbital forcing with results of their study (De Vleeschouwer *et al.*, 2014). In this response, we will provide the maps he had asked for in his comment and several other figures which help to better understand the discrepancy between their and our results. We also thank him for making their data for the heat flux used for calibration as well as the sea-ice data for the median orbit and the minimum and maximum obliquity simulations available to us.

Hereafter, we first have a look at the response of continental snow and sea ice to orbital forcing, as suggested by David De Vleeschouwer. We will then give a short comparison of the median orbit simulations [$\varepsilon = 23.5^\circ$; $e = 0.0$; $\omega = 0^\circ$] of our study and De Vleeschouwer *et al.* (2014), as this is the simulation which is used for the ocean heat flux calibration in De Vleeschouwer *et al.* (2014). Finally, we present and discuss the requested maps showing the surface temperature differences between [$\varepsilon = 23.5^\circ$; $e = 0.069$; $\omega = 90^\circ$] and [$\varepsilon = 23.5^\circ$; $e = 0.069$; $\omega = 270^\circ$].

First, we investigate the response of continental snow to orbital forcing by discussing the differences between [$\varepsilon = 23.5^\circ$; $e = 0.069$; $\omega = 90^\circ$] and [$\varepsilon = 23.5^\circ$; $e = 0.069$; $\omega = 270^\circ$]. The upper panel of Figure 1 shows monthly differences between perihelion in December ($\omega = 90^\circ$) and perihelion in June ($\omega = 270^\circ$) in incoming solar radiation at Earth's surface, snow cover and temperature for the location shown in the lower panel. This figure can be compared to Figure 10 (c) in De Vleeschouwer *et al.* (2014).

The seasonal cycle of these variables in our model agrees very well with De Vleeschouwer *et al.* (2014): Solar radiation differences are negative from June to October, as the Earth receives less solar radiation during this season for perihelion in December. This leads to a slower melting of the Gondwanan snow cover for this orbital configuration which can be seen in the snow cover lines of De Vleeschouwer *et al.* (2014) and our study, showing a maximum in October. The snow albedo effect for perihelion in December is not as strong as observed in De Vleeschouwer *et al.* (2014) in our simulations, visible in the positive radiation difference for November and the earlier increase of temperature differences. However, we note that our location might slightly differ from the one De Vleeschouwer *et al.* (2014) use. We observe other regions further east in Gondwana with a longer persistence of the snow cover. Therefore, we conclude that the models agree very well with respect to the response of continental snow to orbital forcing and that this is not the root cause of the differences between our model results.

In the next step, we investigate the response of sea ice to orbital forcing by looking at the seasonal sea-ice fractions for different obliquities ([$\varepsilon = 24.5$; $e = 0.0$; $\omega = 0^\circ$],

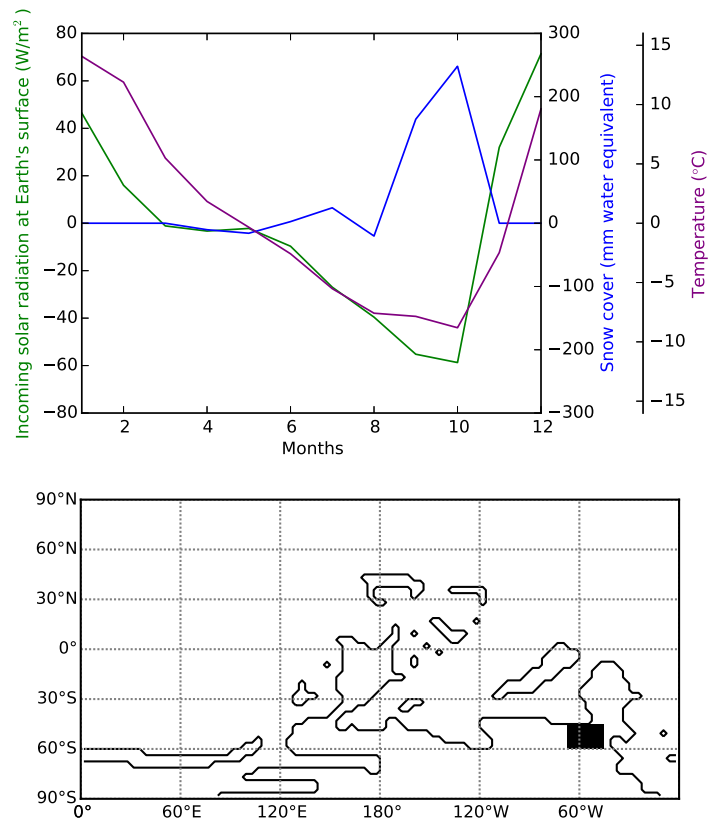


Figure 1: Upper panel: Monthly means for incoming solar radiation, snow cover and surface air temperature at the location on Gondwana shown in the lower panel.

[$\varepsilon = 23.5^\circ$; $e = 0.0$; $\omega = 0$], [$\varepsilon = 22.0^\circ$; $e = 0.0$; $\omega = 0$], Figure 2 to 4) and can compare them with sea-ice distributions in De Vleeschouwer *et al.* (2014) for the same orbital configurations (not shown here), finding significant differences.

As described in De Vleeschouwer *et al.* (2014), they find no sea ice for the obliquity maximum and attribute this to the thermal inertia of the oceans. This is a significant difference to the sea-ice distribution in our simulations (Figure 2): Comparing the Arctic sea-ice fraction of December for the obliquity maximum with the obliquity minimum, we also see the influence of the ocean's thermal inertia, as we have smaller fractions and a smaller extent of sea ice despite a smaller radiative forcing for the obliquity maximum for the Arctic in December. However, in contrast to De Vleeschouwer *et al.* (2014), sea ice does not disappear completely and follows the expected seasonal cycle: Sea ice starts to grow in December, the maximum arises in March due to a time lag caused by the thermal inertia of the oceans, and small fractions are left in June.

For the median orbit case, De Vleeschouwer *et al.* (2014) simulate no sea ice in the SH

and very small fractions for the Arctic. In our simulations, there is sea ice in the SH from June until September, Arctic sea ice reaches its maximum extent in March and shows a typical seasonal cycle (Figure 3).

For the obliquity minimum (Figure 4), we find comparable distributions and fractions for December for our simulation and De Vleeschouwer *et al.* (2014), but the seasonality differs significantly: For the Arctic, sea ice starts to grow in December in our model, reaches its maximum in March, decreases significantly until June and has vanished in September. In De Vleeschouwer *et al.* (2014), in contrast, sea ice starts to grow already in September–October–November (SON), reaches its maximum extent in December–January–February (DJF), recedes to a very small fraction in March–April–May (MAM) and is zero in June–July–August (JJA). In the Southern hemisphere (SH) we simulate sea ice from June until December with a maximum in September, whereas sea-ice fractions are very small in the SH in De Vleeschouwer *et al.* (2014) and increase only from MAM until JJA.

This analysis suggests that the ultimate cause of the differences between our results and De Vleeschouwer *et al.* (2014) results from the ocean/sea-ice components of the respective models. De Vleeschouwer *et al.* (2014) use a simpler mixed-layer ocean model with a heat-convergence term derived from the median orbit configuration and a thermodynamic sea-ice model which allows for free drift (Williams *et al.*, 2001). Our study, on the other hand, is based on an ocean general circulation model (Pacanowski & Griffies, 1999; Montoya *et al.*, 2005) and the two-dimensional, dynamic-thermodynamic sea-ice model by Fichefet & Maqueda (1997) which employs the elasto-viscous-plastic rheology of Hunke & Dukowicz (1997).

Moving on to the second part of our response, Figure 5 shows surface air temperature maps for the median orbit configuration [$\varepsilon = 23.5^\circ$; $e = 0.0$; $\omega = 0^\circ$]. Comparing this to Figure 2 in De Vleeschouwer *et al.* (2014), we see very good agreement. In Figure 6 we compare the ocean heat flux of our model with the one of De Vleeschouwer *et al.* (2014) (not shown) for the median orbit. Here again, we find a good agreement, with some differences on the coasts of Gondwana which might result from the differences in sea ice described above.

As requested in David De Vleeschouwer's comment, Figure 7 shows maps for the surface air temperature differences between perihelion in December [$\varepsilon = 23.5^\circ$; $e = 0.069$; $\omega = 90^\circ$] and perihelion in June [$\varepsilon = 23.5^\circ$; $e = 0.069$; $\omega = 270^\circ$], as in Figure 8 of De Vleeschouwer *et al.* (2014). The patterns over continental areas agree very well, suggesting again that the differences between the two studies are not due to land-albedo or atmospheric effects. In contrast to the agreement over land, however, the temperature differences over the Arctic ocean differ significantly: Arctic differences are negative for all seasons in De Vleeschouwer *et al.* (2014) and have a larger amplitude compared to our results. In our simulations, we have negative Arctic

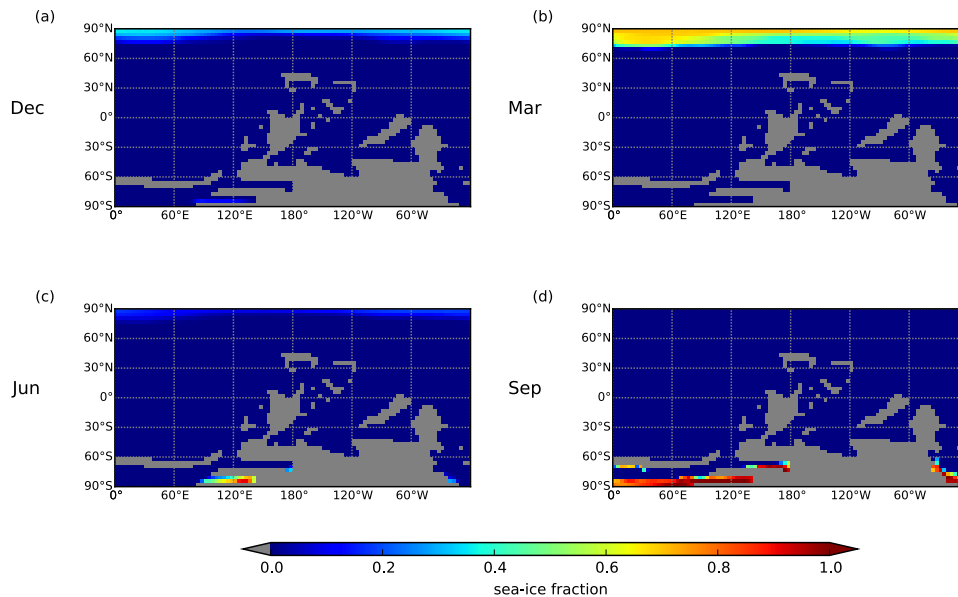


Figure 2: Seasonal sea-ice fraction for $\varepsilon = 24.5^\circ$; $e = 0.0$; $\omega = 0^\circ$. Seasonal values are shown for December (a), March (b), June (c) and September (d) to capture the minima/maxima in the hemispheric sea-ice fractions in spring and autumn.

temperature differences only for MAM and JJA. As for the sea-ice distribution, this might originate from differences in the ocean's inertia which is largely determined by ocean circulation and upwelling. Bearing in mind that we find very good agreement comparing our median orbit simulation's temperatures and heat fluxes, the observed differences for other configurations between our study and De Vleeschouwer *et al.* (2014) might also result from the fact that De Vleeschouwer *et al.* (2014) use the heat flux of the median orbit simulation for all orbital configurations.

Summarising the analysis above, we find generally good agreement for the median orbit simulations of the two models and for patterns over continents. Differences arise for other orbital configurations and for ocean areas, in particular over the Arctic ocean where we find significant differences in the sea-ice distribution between the two studies. Although we are not able to fully explain these discrepancies based on the available data and our understanding of the model used in De Vleeschouwer *et al.* (2014), this strengthens our earlier assumption that these differences arise from differences in ocean circulation, ocean heat flux as well as ocean heat transport and their interplay with sea-ice formation and dynamics. We would like to point out that one would expect these aspects to be captured more realistically in our model configuration.

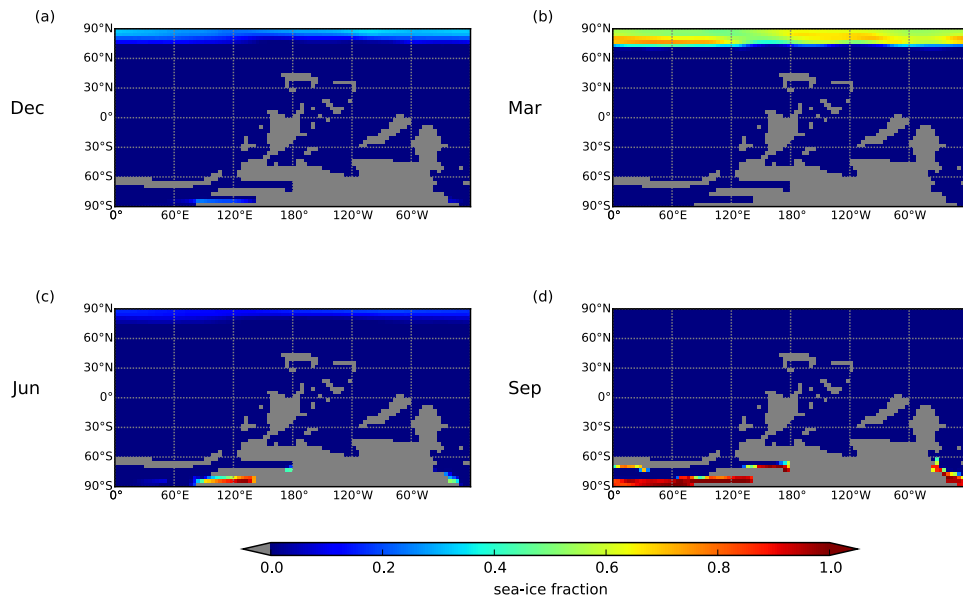


Figure 3: Same as Figure 2, but for $\varepsilon = 23.5^\circ$; $e = 0.0$; $\omega = 0^\circ$.

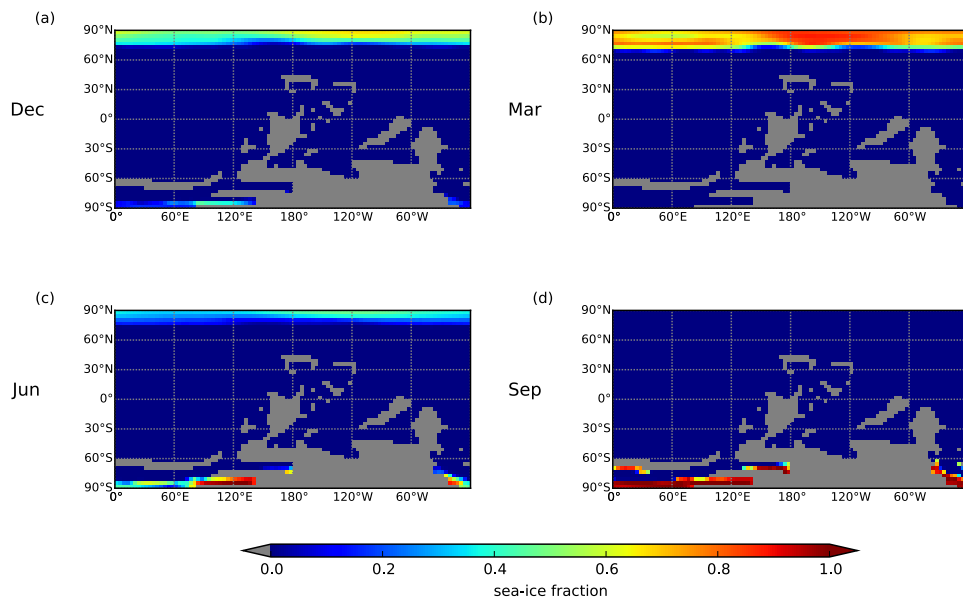


Figure 4: Same as Figure 2, but for $\varepsilon = 22.0^\circ$; $e = 0.0$; $\omega = 0^\circ$.

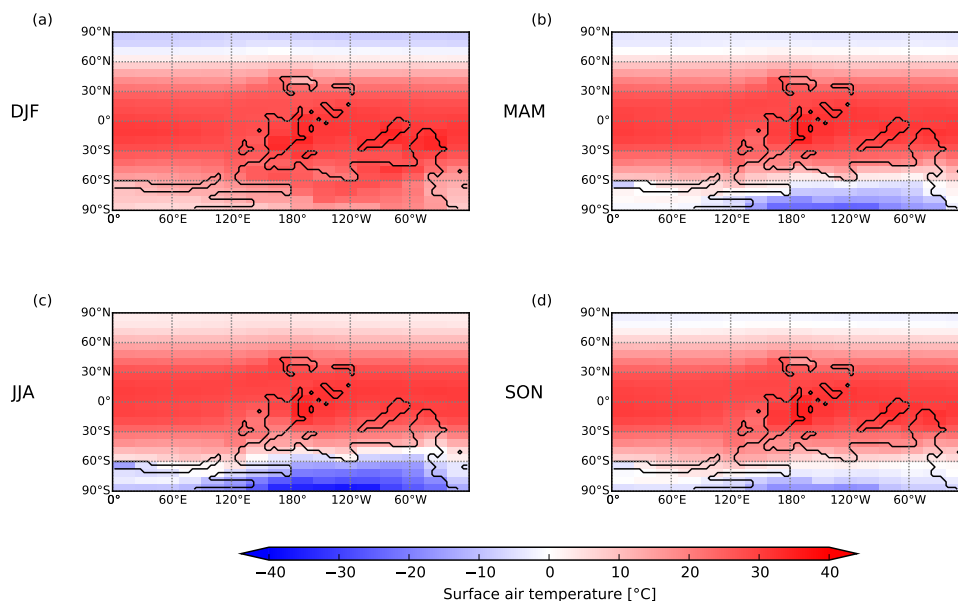


Figure 5: Seasonal surface air temperature maps for DJF (a), MAM (b), JJA (c) and SON (d) in our median orbit simulation, as in De Vleeschouwer *et al.* (2014), Figure 2.

References

- De Vleeschouwer, D., Crucifix, M., Bounceur, N. & Claeys, P. 2014: *The impact of astronomical forcing on the Late Devonian greenhouse climate*, *Global Planet Change*, 120, 65
- Fichefet, T. & Maqueda, M. A. M. 1997: *Sensitivity of a global sea ice model to the treatment of ice thermodynamics and dynamics*, *J. Geophys. Res.*, 102, 12609
- Hunke, E. C. & Dukowicz, J. K. 1997: *An ElasticViscousPlastic Model for Sea Ice Dynamics*, *Journal of Physical Oceanography*, 27, 1849
- Montoya, M., Griesel, A., Levermann, A., Mignot, J., Hofmann, M., Ganopolski, A. & Rahmstorf, S. 2005: *The earth system model of intermediate complexity CLIMBER-3 α . Part I: description and performance for present-day conditions*, *Clim. Dyn.*, 25, 237
- Pacanowski, R. C. & Griffies, S. M. 1999: *The MOM-3 Manual*, Tech. Rep. 4 GFDL Ocean Group, NOAA/Geophysical Fluid Dynamics Laboratory, Princeton, NJ
- Williams, K. D., Senior, C. A. & Mitchell, J. F. B. 2001: *Transient Climate Change in the Hadley Centre Models: The Role of Physical Processes*, *Journal of Climate*, 14, 2659

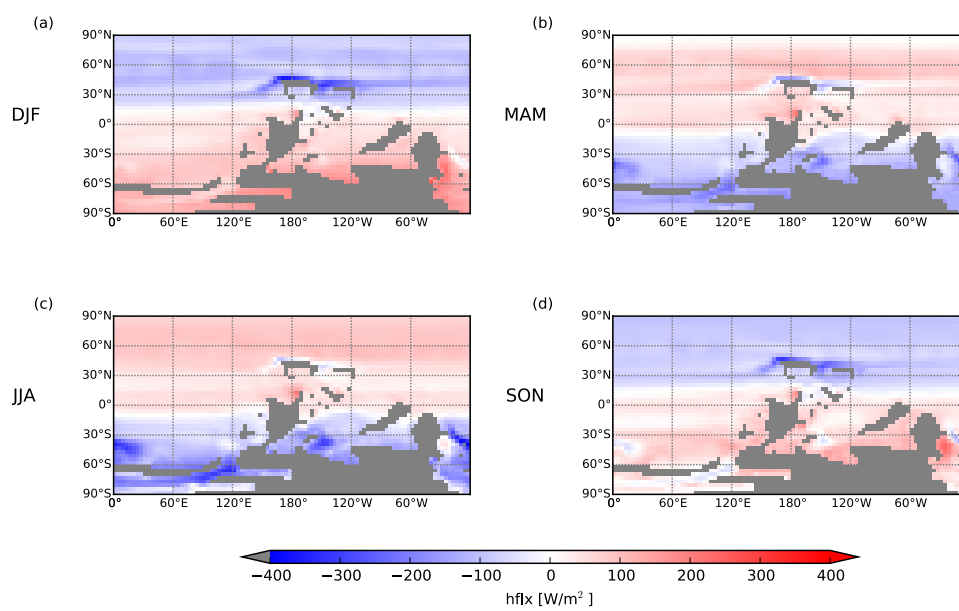


Figure 6: Seasonal ocean surface heat flux maps for DJF (a), MAM (b), JJA (c) and SON (d) in our median orbit simulation.

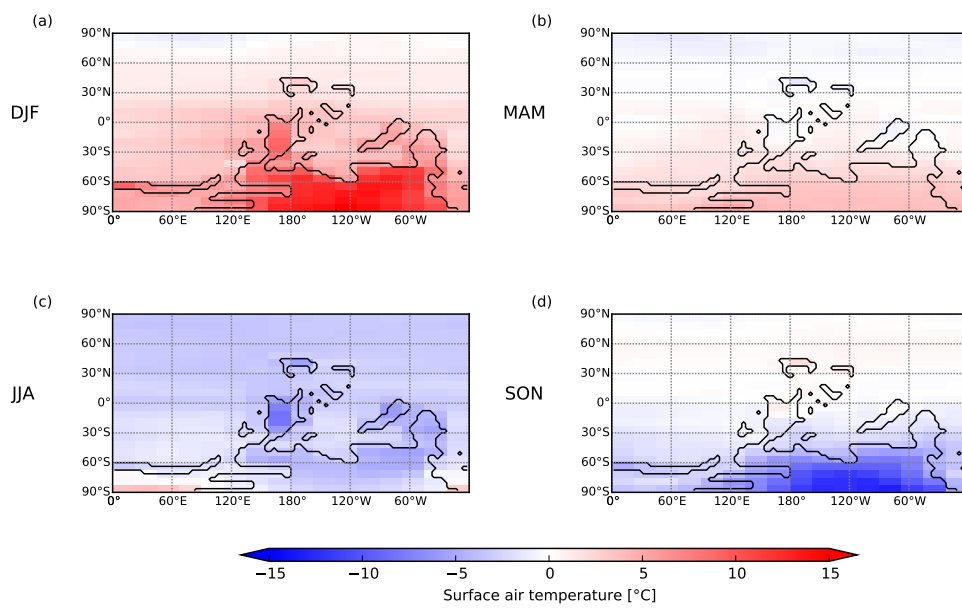


Figure 7: Difference of seasonal surface air temperature for perihelion in December minus perihelion in June for DJF (a), MAM (b), JJA (c) and SON (d).